Rev. Int. Contam. Ambie. 38 (Environmental Science and Policy for Sustainable Development) 117-129, 2023
https://doi.org/10.20937/RICA.54592

AN INTELLIGENT CONTROL METHOD FOR THE SPRAYING AMOUNT OF A SELF-PROPELLED WEEDER BASED ON A DYNAMIC PROGRAMMING ALGORITHM

Un método de control inteligente para la cantidad de pulverización de una desbarbadora autopropulsada con base en un algoritmo de programación dinámica

Dandan ZOU[1], Gang CHE[2]*, Lin WAN[2] and Shiqi LIU[3]

[1] Educational Technology and Information Center, Heilongjiang Bayi Agricultural University, Daqing 163319, China.
[2] College of Engineering, Heilongjiang Bayi Agricultural University, Daqing 163319, China.
[3] Institute of New Rural Development, Heilongjiang Bayi Agricultural University, Daqing 163319, China.

*Author for correspondence: sharpliu0909@126.com

(Received: October 2021; accepted: April 2022)

Key words: Dynamic planning algorithm, path planning, pesticide spraying amount, PID control algorithm.

ABSTRACT

When the self-propelled weeder reaches an obstacle, the amount of pesticide spraying does not change according to the actual situation, leading to an application imbalance. Therefore, an intelligent control method of spraying output of a self-propelled weeder based on a dynamic programming algorithm (DPA) was proposed. The dynamic norm algorithm transformed obstacle avoidance path planning into a multi-stage decision-making problem. The obstacle avoidance path was planned, and the pesticide dosage control equation was designed by using the PID control algorithm to realize the obstacle avoidance and variable application of self-walking weed killer. The experimental results show that the designed self-walking weeder can effectively avoid obstacles, and the maximum average dosage error is 1.4%. Therefore, the method can effectively apply the dosage according to the actual situation and guarantee the balance of spraying quantity.

Palabras clave: algoritmo de planificación dinámica, planificación de rutas, cantidad de pulverización de plaguicidas, algoritmo de control PID.

RESUMEN

Cuando la máquina de deshierbe autopropulsada alcanza un obstáculo, la cantidad de pulverización de plaguicidas no cambia de acuerdo con la situación real, lo que conduce a un desequilibrio de la aplicación. Por lo tanto, se propone un método de control inteligente para la aplicación de rocío de una máquina auto propulsada de deshierbe con base en un algoritmo de programación dinámica. El algoritmo de normas dinámicas transformó la planificación para evitar obstáculos obstáculos en un problema de toma de decisiones en varias etapas. Se planeó la ruta para evitar obstáculos y la ecuación de control de dosificación de plaguicdas se diseñó usando el algoritmo de control PID para identificar los obstáculos y la aplicación variable del herbicida de la máquina. Los resultados experimentales muestran que la máquina de deshierbe auto propulsada puede evitar eficazmente los obstáculos, y el error de dosificación promedio máximo es de 1.4%. Por lo tanto, el método puede aplicar eficazmente la dosis de acuerdo con la situación real y garantizar el equilibrio de la cantidad de pulverización.

INTRODUCTION

The self-propelled weeder mainly comprises a bevel gear commutator, a hydraulic system, a horizontal weeding knife, a vertical weeding knife, an inductive contact rod, and others (Martinez-Sanchez and Jimenez 2019). Due to the increase of agricultural planting scale, the self-propelled weeder cannot be effectively controlled in the spray input, which has become one of the main problems puzzling the growers. In the working of the self-propelled weeder, there are often obstacles that are forced to stop working at a certain place or need more time to break through the obstacles. It is unable to move at the given speed, but the spraying device on the self-propelled weeder will not stop working with it, and it still continues to spray pesticides according to the set rules, which leads to the imbalance of spraying input. There may be too much spraying in a certain area, which leads to excessive pesticide residues and pesticide pollution. Although the purpose of the weeding is achieved, it also may cause huge economic losses. In a word, there are two main reasons for the unbalanced input of self-propelled weeder: one is the path planning and control; the other is that the spraying system is unable to carry out variable application according to the actual situation.

For the above problems, scholars at home and abroad have carried out relevant research. China's self-propelled weeder starts late and the application of related fields is not mature enough, so it mainly depends on foreign imports. Chandel et al. (2018) studied a kind of continuous weeder based on position sensor, digital image processing and single chip microcomputer control, using visual technology. The image analyzer developed by studio open computer vision platform can measure the weed density between crop rows under different light levels. The motion induction of the machine was realized by the inductive proximity switch. The developed system has been calibrated in the laboratory, and then extensive field tests have been carried out. The average weeding efficiency and the plant damage rate was 90.30% and 5.74%, respectively. Based on the literature and experimental experience in weed resistance research, the factors influencing the source of resistance were described. The origin of weed resistance of active components with different action modes was introduced in chronological order, and the distribution of weed resistance in the world was summarized (Chodová et al. 2018). Wen et al. (2019) studied the effects of a new type of gas assisted electric knapsack sprayer and two conventional knapsack sprayers on the settlement, residue and loss of pesticides in soil. The sediment collected from the six areas on the surface of the blade was collected and analyzed by liquid chromatography triple four pole mass spectrometry (Chen et al. 2020). The results show that the air assisted electric backpack sprayer is better than the traditional one. The fog method has a large amount of deposition, good permeability and uniformity (Wen et al. 2019). Forcella et al. (2018) carried out field test with abrasive sand driven by compressed air, and treated the annual weed seedlings growing at the base of corn plants in summer at different early stages of leaf development. Lv et al. (2019) with wireless cache nodes, optimized the downlink transmission scheduling of popular files. Without active multicast, the problem of downlink transmission resource minimization was described as a dynamic programming problem with random stages which could be approached by a finite level Markov decision with fixed stages. A low complexity degree scheduling strategy was proposed through linear approximation to the value function of MDP, thus obtaining the bound of approximation error (Zuo et al. 2020, He et al. 2021). However, due to the poor path planning effect and high error of pesticide spraying amount, this method has limitations and poor overall control effect.

Based on the above research background, this paper takes the dynamic planning algorithm as the core to solve the path planning control problem of the self-propelled weeder. Then it combines the fuzzy PID control algorithm to real-time control the dosage changes according to the self-propelled weeder's moving state, so as to balance the dosage control.

The intelligent control method of spraying dosage of self-propelled weeder

The self-propelled weeder can effectively solve the harm of diseases, insects, and pests to crops in the application to reduce farmers' economic loss. There is no permanent weeding method, and a self-propelled weeder cannot achieve endless weeding, only to slow down the growth of weeds as much as possible. The commonly used weeding methods are generally manual removal, electric current weeding, flame weeding, photochemical weeding, herbicide, film weeding, and others, which can effectively remove weeds. Spraying herbicide with a weeder is the most common method among all weeding methods. The self-propelled weeder mainly comprises a frame assembly, gasoline engine, transmission system, walking system, protective cover, gearbox, control system, depth limiting mechanism, and weeding wheel (Kim et al. 2017) as shown in **figure 1**. The working principle of self-propelled weeder is that when it drives to the target working area, the treatment tank with the prescribed dose of liquid is filled, then the rear wheel track is adjusted according to the ridge and ditch distance of the working area, the spraying rack is expanded to a fixed position, and it is lifted to a suitable working height. The spraying machine starts and enters the target working area to spray the target crops after the operation of each mechanism and spraying system is stable. After the work is completed, it needs to close the spraying system, restore the spraying rack to the initial position and the rear wheel spacing to the safe driving distance of the road, and drive out of the target working area to complete the spraying operation in the target area (Yu et al. 2020).

The self-propelled weeder can generally remove 80%-90% of the weeds, and some can remove 100%. The weeding is very thorough. It can kill the common annual and perennial weeds, and the cost is one thirtieth or one twentieth of the manual weeding. It can reduce the weeding cost and improve the labor production rate. However, because the weeder mainly implements the non-variable application control, the application amount is subject to the unit's moving state. To a certain extent, it will lead to unreasonable use of pesticides and excessive pesticide residues, damage or even kill other plants and pollute the environment. To solve the improper injection of self-propelled weeder, the path planning and control of self-propelled weeder should be studied.

Path planning control of self-propelled weeder

The path planning of self-propelled weeder is to find a moving path from a given starting point to a given target point in the work environment with obstacles, so that it can safely bypass all obstacles without collision in the work, and try to meet the optimization indicators such as the shortest time and the lowest energy consumption. According to the different understanding of self-propelled weeder

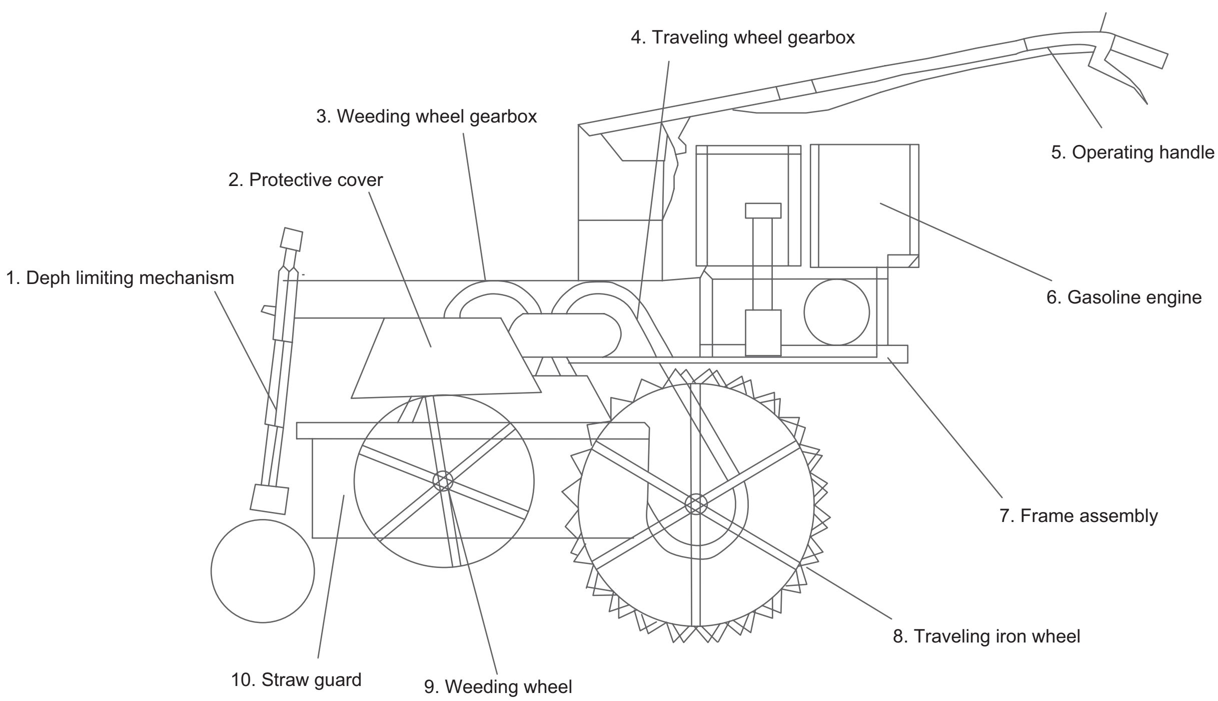

Fig. 1. Structure of self-propelled weeder.

to environmental information, path planning can be divided into two types: one is the global path planning with fully known environmental information, also known as static or offline path planning; in the other the environmental information is completely unknown or partially unknown, and the working environment of self-propelled weeder is detected online through sensors to obtain the location of obstacles. Local path planning with shape and size information is also called dynamic or online path planning.

In this paper, the dynamic norm algorithm was used to transform the obstacle avoidance path planning into a multi-stage decision-making problem, thereby effectively combining the problem with dynamic programming. For each stage of the subproblem, equation (1) is applied and the shortest path of each stage and the global optimal solution are obtained (Perazzo et al. 2017).

$$\psi_{a.t}(t) = a^{-\frac{1}{2}}\psi\left(\frac{t-\tau}{a}\right), a > 0, \tau \in R \tag{1}$$

Where $\psi_{a.t}(t)$ is the solution function, a is the dynamic planning factor, τ is the translation factor, and t is the independent variable of the solution function.

Compared with the previous algorithms, the dynamic norm algorithm can effectively reduce the calculation amount while getting the global optimal solution (He et al. 2019), and the whole analysis and solution is simple and clear. By introducing DPA, the obstacle avoidance path is planned.

Introducing DPA

The DPA is used to decompose the problem to be solved into several subproblems, and then the solution of the substage and the former problem is obtained in turn, which provides useful information for solving the latter problem. When a subproblem is solved, all kinds of possible local solutions are given. By judging which of them can reach the optimal solution, other local solutions are abandoned. Each subproblem is solved in order, and the last subproblem is the initial solution. The dynamic programming in the design has a certain mode, which generally goes through several steps as shown in **figure 2**.

(1) According to the characteristics of time and space, the problem is divided into several stages. When segmenting, it needs to note that the segments must be orderly or sortable, otherwise the problem cannot be solved.
(2) Determining state and state variables. The objective conditions under which a problem develops to different stages are expressed in different states. It is true that the selection state should meet the requirement of no after effect.
(3) Determining the decision and writing out the state transition equation. Because there is a natural connection between the decision and the state transition, the state transition is to derive the state of this stage according to the state and decision of the previous stage. So, if this is true, the state transition equation is written down. However, in practice, it is often the opposite. According to the state relations of the two adjacent stages, the decision-making method and the state transfer equation are determined.
(4) Looking for boundary conditions. The state transfer equation given is recursive, which requires a recursive end condition or a boundary condition.

Generally speaking, the state transition equation (including boundary conditions) can be written as the stage, and state transition decision-making of solving problems (Chandel et al. 2018).

In practical application, DPA can be introduced in the following steps:

(1) This paper analyzes the properties of the optimal solution and characterizes its structure.
(2) Defines the optimal solution of recursion.

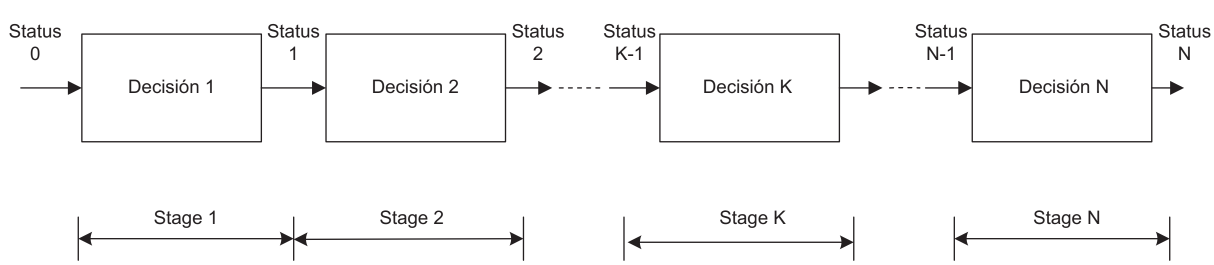

Fig. 2. Schematic diagram of dynamic programming decision process 1.

(3) The best value is calculated from the bottom up or from the top down by memory method (memo method).
(4) The optimal solution of the problem is constructed according to the information obtained from the calculated optimal value.

The main difficulty of DPA is the theoretical design, that is, the determination of the above four steps; once introduced, the implementation part will become very simple. To solve the problem with dynamic programming, three elements should be determined first: (1) problem stage; (2) state of each stage; (3) recurrence relationship between the previous stage and the next stage. Recurrence relation is a kind of transformation from a small problem to a large problem. In this case, dynamic programming can often be realized by recurrence method. However, because recurrence method can make full use of the solutions of existing subproblems and reduce repeated calculation, it has incomparable advantages for large problems, which is dynamic programming the core of law (Cheng et al. 2018).

When these three elements of dynamic programming are determined, the whole solution can be described by an optimal decision table, that is, a two-dimensional table, in which the row represents the decision-making stage and the column represents the state of the problem. The data required to fill in the table generally corresponds to the optimal value of a problem at a certain stage (such as the shortest path, the longest common subsequence, the maximum value, etc.). The filling is based on the recurrence relationship. From row 1 and column 1, it fills in the table in order of row or column priority, and finally fills the whole data in the whole table into the optimization table through simple selection or operation.

Obstacle avoidance path planning

On the basis of DPA, the obstacle avoidance path planning was carried out (Li, 2019). It needs to bypass obstacles when the target cannot be reached in a straight line. Therefore, it can be regarded as a multi-stage decision-making problem based on the obstacles encountered in the solution. The path planning problem is transformed into a multi-stage decision-making problem, which is solved by dynamic programming. Therefore, according to the solution idea of dynamic programming, it first plans the solution environment, then solves the problem by stages according to the distribution of obstacles, and then determines the state points of each stage (Barré et al. 2018). The planning of obstacle avoidance path is as follows:

Step 1: Solve the working environment of self-propelled weeder.

The visual graphic method is to transform all the real obstacle sets into polygon sets on the plane, and expand the corresponding points of the starting and the ending point into polygon sets. The size of the robot is extended to the boundary of the obstacle, so that the self-propelled weeder can be considered in the solution environment as shown in **figure 3**. In addition, in the equivalent figure, the concave part of the polygon becomes a convex polygon by connecting its vertices, thus reducing the calculation amount without affecting the solution result (Wang et al. 2018). Therefore, a solution environment can be constructed by taking the self-propelled weeder as a point, at the same time, the obstacle is equivalent to a convex polygon set in the plane, and the starting point and target point in the space are extended to a polygon set.

Step 2: Divide obstacle avoidance path planning stage.

According to the number of obstacles bypassed in the path, the number of stages is divided, and the decision-making is made for each stage to achieve the best effect in the whole process. As shown in **figure 3(a)**, the obstacles are divided into N stages from the starting point to the target point.

When two obstacles are side-by-side, or parallel and X-axis lines are made in the coordinate diagram, if this line can have two or more obstacles at the same time, these obstacles are regarded as the same stage, as shown in **figure 3(b)**. Among them, A is the starting point, O is the target point, I is the obstacle in the first stage and II is the obstacle in the second stage.

Step 3: Determine the status points in each stage.

In the path planning of the self-propelled weeder, the determination of the state points in each stage is the determination of the vertex of the obstacle (convex polygon), as shown in **figure 4**.

Through the study of each stage of path planning of the weeder, the following provisions are made for the determination of state points in each stage:

1) Taking the starting point as the source point of path planning is to make a tangent line for each obstacle in the working of the weeder, and the tangent point must be the state point.

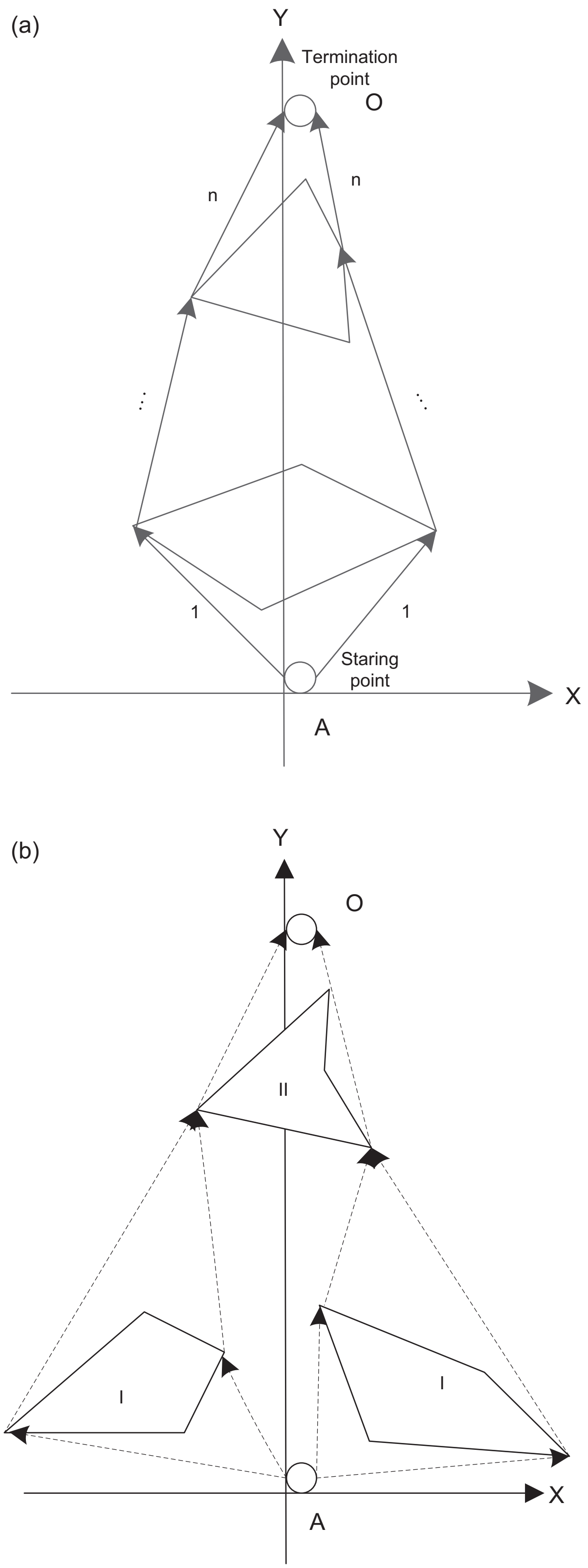

Fig. 3. Obstacle division. (a) Stage division of serial obstacles, (b) stage division of parallel obstacles.

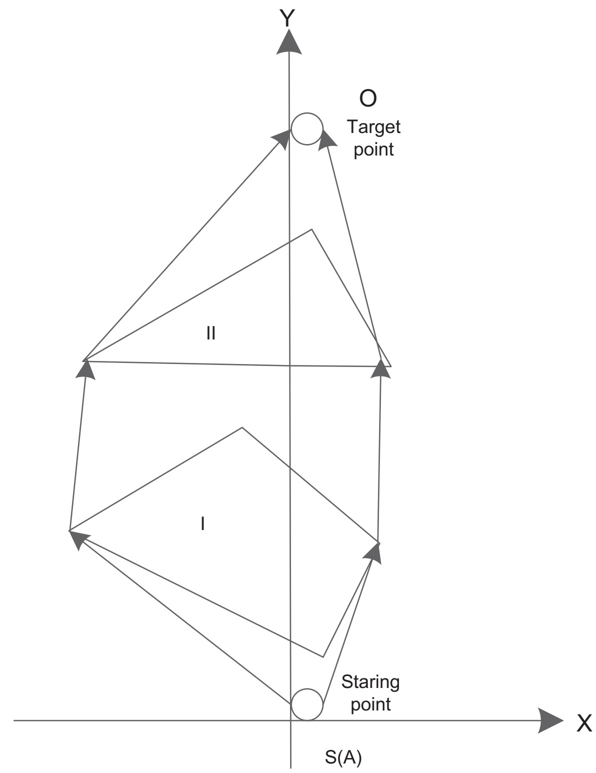

Fig. 4. Determination of state points in each stage.

2) It takes stage I as the research object and draws a straight line from the determined state point to the target point. If it can reach the target point directly, then the subsequent marked state points on this side can be omitted. If it is not direct, it will not be dealt with.
3) Taking stage II as the object, the determined state point is used as a straight line to the state point marked in the last stage. If it can reach directly, the subsequent marked state points on this side are omitted. If it is not direct, it will not be dealt with.
4) For the two adjacent obstacles, as shown in **figure 5**, it first defines whether the determined state points B1 and B2 can reach in straight line with C1 and C2 respectively. If they can, then other state points need not be determined, as shown in **figure 5(a)**. If they cannot, then it determines which side of the convex polygon the line intersects, and connects the two vertices of the intersecting edge. For example, in **figure 5(b)** the broken line b1b3c2 is formed by connecting the vertex B3 and the vertex C2 near B1, and then marks point B3 as the state point.
5) Repeat steps 2), 3) and 4) from stage II to the last stage.

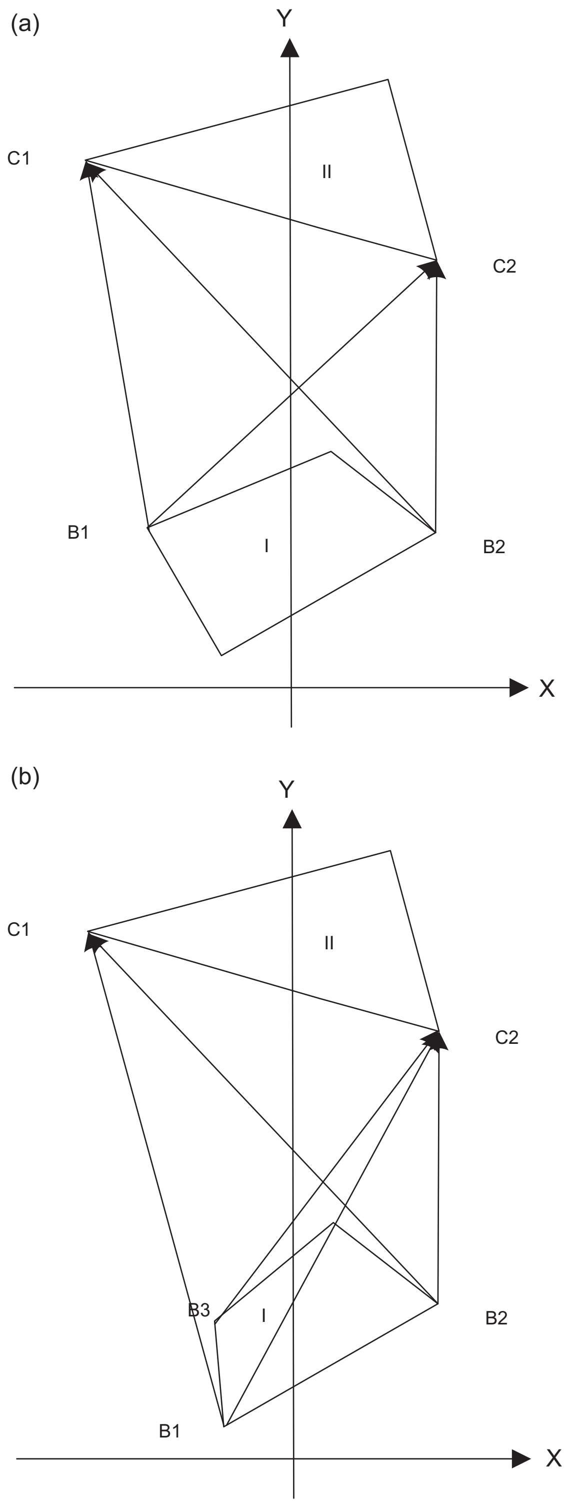

Fig. 5. Schematic diagram of shortest path solution between adjacent phase state points. (a) The shortest path when the adjacent obstacle state point can reach directly, (b) the shortest path when the adjacent obstacle state point cannot reach directly.

Variable application control of spraying system

The function of the treatment box of the self-propelled weeder is to store the treatment liquid, which is an indispensable part of the operation of the spraying machine. Therefore, the degree of automation of the treatment box is also one of the important factors to determine the performance of the spraying machine. The whole system constitutes a complete closed circuit (Takayanagi et al. 2018). The control system block diagram is shown in **figure 6**.

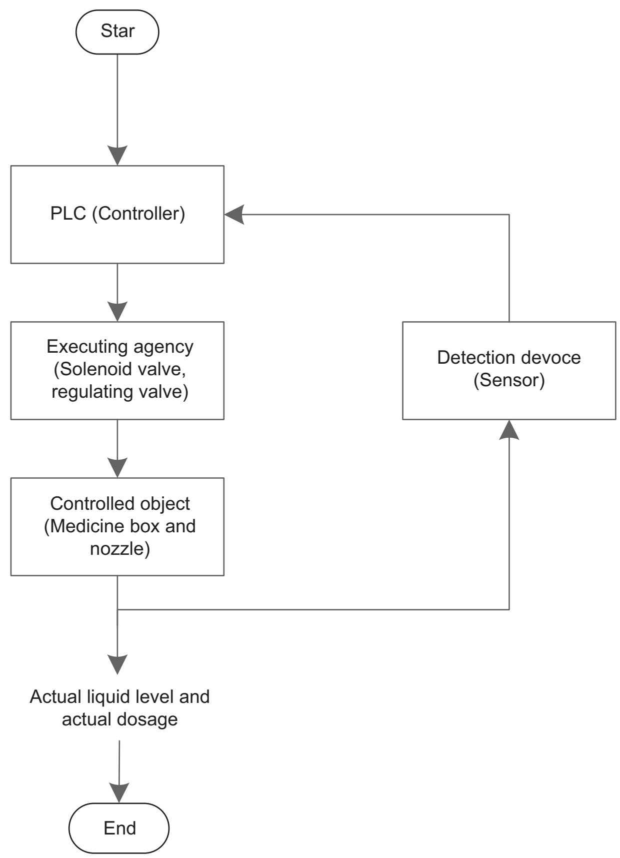

Fig. 6. Control system block diagram.

The overall structure of the spray box control system includes treatment box, aeration solenoid valve, liquid supply electromagnetic valve, liquid level sensor, filter, spray pump, overflow valve, electric control valve, pressure sensor, flow sensor, sprinkler head, spraying solenoid valve, PLC and touch screen (Sundar et al. 2019, Cao 2020). The core component of the system uses PLC as the controller. Various solenoid valves and regulating valves are executive components, which are respectively responsible for adding treatment solution to the tank and regulating the flow rate of the solution in the tube. The controlled object is the treatment box and the sprayer, which are used to store and spray the liquid respectively. Liquid level sensor, pressure sensor and flow sensor are monitoring elements and system feedback links. They feed the liquid level height and liquid flow information in the treatment tank to PLC in real time.

The application amount is controlled based on the speed of spray machine and the spray amount of spray nozzle to ensure that the application amount per unit area remains the same (Matsuda et al. 2018). The expression of the dosage per unit area is as follows:

$$q = \frac{3.6 \cdot 10^3 np}{vb} \tag{2}$$

In the equation (2), q is the spraying amount of liquid treatment per hectare; p is the spraying amount of single nozzle per minute; v is the speed of the spraying machine during operation; b is the distance between nozzles; n is the number of nozzles.

According to equation (2), when the distance between sprayers b and the number of sprayers n are set during the operation, the driving speed v and the spraying amount per minute of a single sprayer can be controlled to ensure that the spraying amount per unit area is constant.

In the treatment tank control system, the liquid level of the tank is controlled by the switch of the solenoid valve. The system is a non-linear control system, and the model diagram is shown in **figure 7**.

It is set that the actual liquid level value of the spray tank is represented by h, the opening and closing state of the solenoid valve is represented by X, the rising and falling state of the liquid level of the spray tank is represented by Y, and the upper and lower limits of the alarm liquid level value are represented by $H1$ and $H2$. When y = 1 and y = 0, it respectively means the liquid level of the treatment tank is in the rising stage and in the falling stage. When x = 1 and x = 0, it respectively means the liquid level control solenoid valve is in the open state and in the closed state.

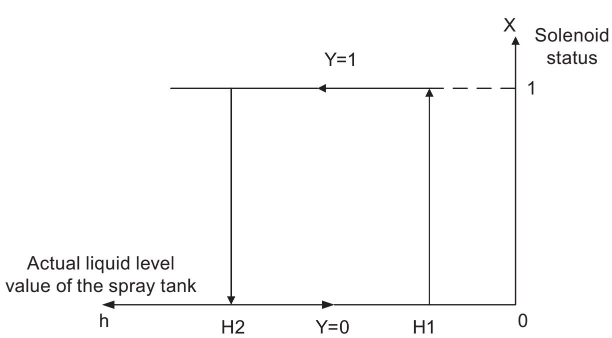

Fig. 7. Control system model.

In the treatment box system, the working state of the solenoid valve is only open and closed (Kim and Lee, 2018). It can be expressed in digital form. When the liquid level value of the treatment tank is lower than the lower limit *H1* of the alarm liquid level value, the solenoid valve open and the system begins to make up water. At this time, the output of the solenoid valve is x = 1; When the liquid level value of the treatment tank is higher than the upper limit *H2* of the alarm liquid level value, the solenoid valve close and the system stops making up water. At this time, the output of the solenoid valve is x = 0.

When the liquid level of the treatment tank is in the rising stage, the solenoid valve is always in the open state. Until it is higher than the upper limit, the solenoid valve can be closed. When the liquid level of the tank is in the falling stage, the solenoid valve is always in the off state. Until it is lower than the lower limit, it can be converted into a mathematical expression, which can make the chart clearer (Zhao et al. 2018).

The mathematical model is established according to the opening and closing state of the control solenoid valve (Wang et al. 2020). The mathematical expression of the system model is as follows:

When x = 1, the solenoid valve is in the open state.

$$Y = \begin{cases} 1, h < H_2 \\ 0, h \geq H_2 \end{cases} \tag{3}$$

When x = 0, the solenoid valve is closed.

$$Y = \begin{cases} 1, h < H_1 \\ 0, h \geq H_1 \end{cases} \tag{4}$$

A reasonable and effective system control algorithm is an important guarantee for variable rate application. In this paper, PID control algorithm and DPA are selected to study the path planning of obstacle avoidance.

PID control algorithm only needs to adjust the proportion coefficient α, integral coefficient β and differential coefficient α of the deviation (Zhao et al. 2018). A kind of linear controller with ideal results can be called PID controller. The closed-loop feedback control is adopted for the control of the dosing amount in the dosing box control system. According to the control deviation $e(t)$ composed of the set dosing amount $q(t)$ and the actual output dosing amount $p(t)$, the deviation is first linearly combined by PID control to form the control amount, so as to obtain the control equation of the system (Tan et al. 2018).

The control equation is:

$$e(t) = q(t) - p(t) \tag{5}$$

The control of the spraying amount of the treatment box is determined by the opening of the solenoid valve which is controlled by the control voltage signal. In the transportation of liquid treatment, because the length of pipeline makes the signal delay in the output, it is necessary to find out the delay function of the system (Lee et al. 2020). The delay transfer function can be expressed as:

$$f(s) = e^{-ts} \approx \frac{1}{1+ts} \tag{6}$$

Where $f(s)$ is the delay transfer function and ts is the total delay time.

To sum up, when the control signal changes, the corresponding dynamic of the valve can be approximately represented by integral link and delay link. Then its transfer function is expressed as:

$$F_e(s) = \frac{R}{1+ts} \tag{7}$$

In the equation, $F_e(s)$ is the transfer function of the actuator of the electric control valve; R is the ratio coefficient of the flow rate and power on time of the electric control valve.

In this paper, PID control algorithm was used to control the dosage (Chen et al. 2018), and the specific process is shown in **figure 8**.

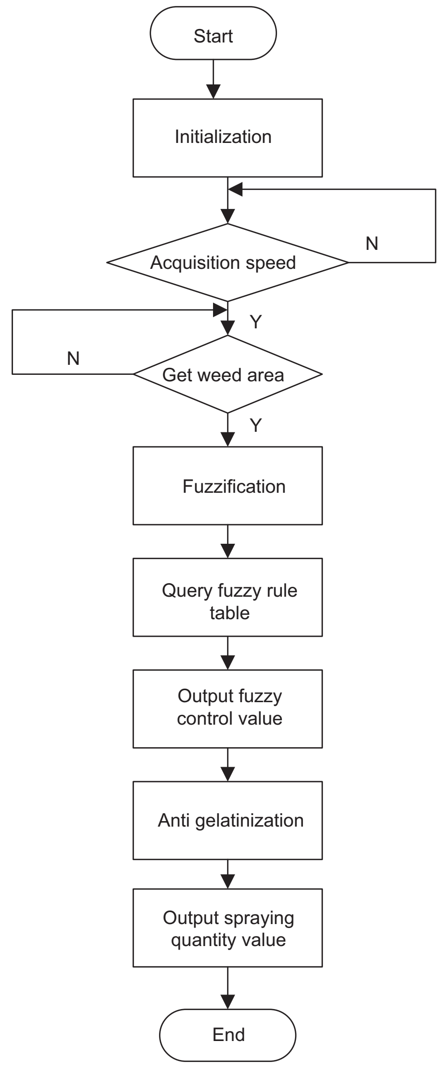

Fig. 8. PID control algorithm control dosing flow.

EXPERIMENTAL ANALYSIS

To verify the rationality of the intelligent control method of spray input of the self-propelled weeder, the spx3150 self-propelled weeder prototype was taken as the research object, and the method proposed in this paper was verified in the Matlab simulation environment. The overall scheme of the experiment was firstly to introduce the research object and experimental parameters, secondly to build simulation scenes, then to design experimental performance indicators, and finally to analyze the performance of the design method according to the performance indicators.

Experimental objects and parameters

This paper used the automatic weeder produced by Casecorp as the control object, as shown in **figure 9**. The spx3150 spray machine was powered by a 6-cylinder 152 horsepower turbocharged diesel

Fig. 9. SPX3150 self-propelled weeder.

engine, driven by four-wheel hydrostatic pressure, with adjustable wheel spacing and high ground clearance. The spray system was equipped with a 3785 treatment box and a 265 cleaning box. On the basis of ensuring large capacity, timely cleaning of the treatment box and the pipeline ensured the service life. The spray head of the equipment is controlled by pulse solenoid valve. The flow controller and nozzle control the number of drug drops. Controlling the size of drug drops through the system pressure and the nozzle can ensure the accuracy of spraying. The main technical parameters of self-propelled weeder are shown in **table I**.

TABLE I. TECHNICAL PARAMETERS OF SPX3150 SELF-PROPELLED WEEDER.

Parameter	Numerical value
Overall dimension (L × w × h)	1570×915×990mm
Rated engine speed	1800 r/min
Auxiliary power	4.05kW
Number of weeding lines	ine#2
Width of one side weeding	160mm
Weeding depth	20-40mm
High speed of weeding rotation	415 r/min
Low speed of weeding rotation	252 r/min
Operation speed	0.4-0.8 m/s

Before the simulation experiment, we first initialized the simulation program, set its initial value to 0, and imported the technical parameters of the self-propelled weeder into the simulation program one by one to ensure the authenticity.

Simulation scene establishment

The simulation scene is shown in **figure 10**, in which the black shadow part is the obstacles encountered by the self-propelled weeder in moving, and the initial position of the self-propelled weeder is at the lower left corner.

Experimental performance index

To verify the feasibility and effectiveness of the design method, different scenarios analysis experiments were designed, according to the balance of self-propelled weeder and the purpose of the pesticide use and effective obstacle avoidance. At the rate of self-propelled weeder as a variable, pesticide used average error for experimental performance indicators. Pesticide consumption after the average error was that pesticide dosage of actual amount minus the

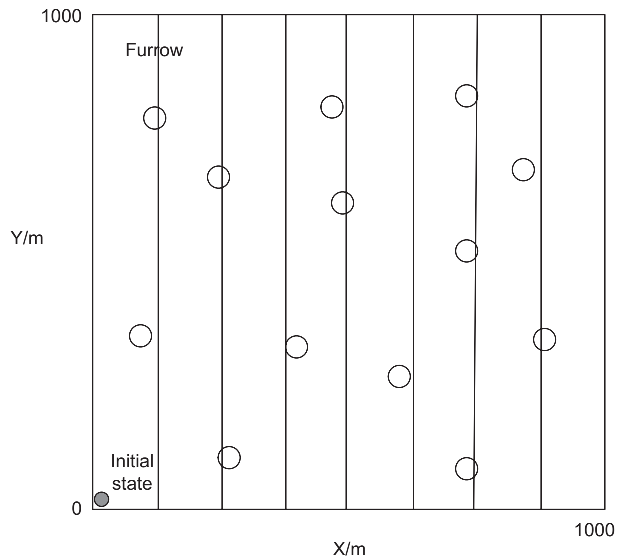

Fig. 10. Simulation scene.

theory of absolute value than the average of the theory on the dosage. The equation of average error is:

$$K = \frac{|K2 - K1|}{K1} \tag{8}$$

In the equation (8), $K1$ represents the theoretical pesticide dosage; $K2$ represents the actual pesticide dosage.

The lower the average error of pesticide dosage, the better the performance of the design method.

Constant speed test and acceleration test

1) Constant speed test

Constant speed test is to verify the change of the actual dosage of the spraying system under different steady speed. The working speed of the sprayer was 0.6 km/h. This paper took 1 km/h, 2 km/h, 3 km/h and 4 km/h as working conditions to test. The width of the sprayer was 6.5 m, the test distance was 200 m, and the application pressure was 0.3 MPa. The test was repeated 20 times, and the average value of the test results was considered. The constant speed test is shown in **table II**.

From the experimental results in **table II**, under the condition of not providing acceleration for the self-propelled weeder, the highest average error of the design method was only 0.9%, and the lowest was 0.3%, and part of the actual dosage was lower than the theoretical dosage. Therefore, the self-propelled weeder spray output control method based on the DPA can effectively control the spray output of the

TABLE II. CONSTANT SPEED TEST RESULTS.

Working condition	Speed (km/h)	Acceleration (m/s^2)	Theoretical dosage (L/hm^2)	Actual dosage (L/hm^2)	Average error (%)
Constant speed test 1	1	0	224	223.3	0.3
Constant speed test 2	2	0	180	180.8	0.4
Constant speed test 3	3	0	120	121.1	0.9
Constant speed test 4	4	0	95	94.5	0.5

weeder. The actual spray output obtained by simulation was relatively low, which was quite different from the theoretical dose. Reducing the spray output also save a lot of economic costs for agriculture households.

2) Accelerated test

In the actual working condition, the moving speed of the spraying machine is changed in real time, and the change of the speed has a great influence on the actual application. In the operation, the speed of the sprayer changed little, and the acceleration was below 0.4 m/s^2. The critical acceleration (0.1 m/s^2 and 0.4 m/s^2) was taken as the working condition in the test. The width of the sprayer was 6.5 m, the test distance was 200 m, and the application pressure was 0.3 MPa. The test was repeated 20 times, and the average value of the test results was considered. The accelerated test is shown in **table III**.

According to the analysis in **table III**, the weeder was stable in field operation, flexible in turning without tipping over, and the adjustment of rear wheel track met the requirements of use. In addition, the average error of pesticide spraying amount was only 1.4%, and the maximum difference of the actual amount was 2.7 L/hm^2. Therefore, the error value is small, meeting the actual demand. It can warrant the balance of synchronous operation of the spraying output, the spraying system, and the spraying machine.

(3) Deceleration test

In the actual work, the speed of the spray machine will sometimes become smaller, which has a great impact on the actual application. In the operation, the speed of the sprayer changed little, and the acceleration was below -0.2 m/s^2. The critical acceleration (-0.1 m/s^2 and -0.2 m/s^2) was taken as the working condition in the test. The width of the sprayer was 6.5 m, the test distance was 200 m, and the application pressure was 0.3 MPa. The test was repeated 20 times, and the average value of the test results was considered. The deceleration test is shown in **table IV**.

According to **table IV**, when the self-propelled weeder run at the same speed, different acceleration values were provided for the weeder which worked normally without failure. The average error of pesticide dosage of spraying system was between 1.2% and 1.4%, the highest average error was only 1.4%, and the highest error dosage was only 2.7 L/hm^2. Therefore, the error of this method is small, and

TABLE III. ACCELERATED TEST RESULTS.

Working condition	Speed (km/h)	Acceleration (m/s^2)	Theoretical dosage (L/hm^2)	Actual dosage (L/hm^2)	Average error (%)
Acceleration test 1	1-4	0.1	190	192.7	1.4
Acceleration test 2	1-4	0.4	190	187.4	1.4

TABLE IV. DECELERATION TEST RESULTS.

Working condition	Speed (km/h)	Acceleration (m/s^2)	Theoretical dosage (L/hm^2)	Actual dosage (L/hm^2)	Average error (%)
Acceleration test 1	1-4	-0.1	190	187.3	1.4
Acceleration test 2	1-4	-0.2	190	192.2	1.2

it can also meet the actual demand in the case of acceleration. It can still be considered that spraying system and spraying machine run synchronically and ensure the balance of spraying input of self-propelled weeder.

CONCLUSION

To improve the efficiency of plant protection and the effective use of pesticides, and to ensure food safety and sustainable development of agriculture as the background, this paper studied the spray output of a self-propelled weeder. The experimental research on the physical prototype showed that the matching error between the spraying system and the spraying machine was in the range of 0.3%-1.4%, which met the requirements. Under the control method based on the DPA, the spraying output of the self-propelled weeder was more balanced. Due to the time limitation, this paper did not conduct in-depth research on the operating efficiency of the algorithm. Therefore, in the follow-up work, the focus must be on this aspect to improve the work efficiency and optimize the control method.

ACKNOWLEDGMENT

Key Laboratory of Intelligent Equipment for Agricultural Machinery in Heilongjiang Province; National Science and Technology Support Key R&D Program (No. 2017YFD04C1203); Heilongjiang province application technology research and development plan major project (No. GA15B402).

REFERENCES

Barré K., Le Viol I., Julliard R. and Kerbiriou C. (2018). Weed control method drives conservation tillage efficiency on farmland breeding birds. Agriculture Ecosystems & Environment 256, 74-81. https://doi.org/10.1016/j.agee.2018.01.004

Cao L. (2020). Changing port governance model: Port spatial structure and trade efficiency. Journal of Coastal Research 95(sp1), 963. https://doi.org/10.2112/SI95-187.1

Chandel A.K., Tewari V.K., Kumar S.P., Nare B. and Agarwal A. (2018). On-the-go position sensing and controller predicated contact-type weed eradicator. Current Science 114(7), 1485-1484. https://doi.org/10.18520/cs/v114/i07/1485-1494

Chen L.H., Reidl F., Rossmanith P. and Villaamil F.S. (2018). Width, depth, and space: tradeoffs between branching and dynamic programming. Algorithms 11(7), 98. https://doi.org/10.3390/a11070098

Chen Y.L., Chen X.J., Zhang C.L. and Deng L.S. (2020). Conversion of ammonium polyphosphate (APP) in acidic soil and its effect on soil phosphorus availability. Applied Ecology and Environmental Research 18(3), 4405-4415. https://doi.org/10.15666/aeer/1803_44054415

Cheng A.T., Zamorano-Sánchez D., Teschler J.K., Wu D. and Yildiz F.H. (2018). NtrCadds a new node to the complex regulatory network of biofilm formation and VPS expression in vibrio cholerae. Journal of Bacteriology 200(15), e00025-18. https://doi.org/10.1128/JB.00025-18

Chodová D., Mikulka J., Kočová M. and Salava J. (2018). Origin, mechanism and molecular basis of weed resistance to herbicides. Plant Protection Science 40(4), 151-168. https://doi.org/10.17221/463-pps

Forcella F., Humburg D., Wortman S.E. and Clay S.A. (2018). Air-propelled abrasive grit can damage the perennial weed quackgrass. Canadian Journal of Plant Science 98(4), 963-966. https://doi.org/10.1139/cjps-2017-0291

He Z., Zhou F., Xia X. and Wen F.H. (2019). Interaction between oil price and investor sentiment: nonlinear causality, time-varying influence, and asymmetric effect. Emerging Markets Finance and Trade 55(12), 2756-2773. https://doi.org/10.1080/1540496X.2019.1635450

He G., Liu X. and Cui Z. (2021). Achieving global food security by focusing on nitrogen efficiency potentials and local production. Global Food Security 29, 100536. https://doi.org/10.1016/j.gfs.2021.100536

Kim H.S., Hong B.G. and Moon S.Y. (2017). Thick tungsten layer coating on ferritic-martensitic steel without interlayer using a DC vacuum plasma spray and a RF low pressure plasma spray method. Thin Solid Films 623(FEB.1), 59-64. https://doi.org/10.1016/j.tsf.2016.12.049

Kim K. and Lee K.M. (2018). Dynamic programming-based vessel speed adjustment for energy saving and emission reduction. Energies 11(5), 1273. https://doi.org/10.3390/en11051273

Lee H.J., Kim H.S., Park J.M., Cho H.S. and Jeon J.H. (2020). PIN-mediated polar auxin transport facilitates root−obstacle avoidance. New Phytologist 225(3), 1049-1052. https://doi.org/10.1111/nph.16076

Li M. (2019). Simulation of obstacle avoidance trajectory for lidar detection of gliding vehicle. Computer Simulation 36(6), 55-58. https://doi.org/10.3969/j.issn.1006-9348.2019.06.011

Lv B.J., Huang L.X. and Wang R. (2019). Joint downlink scheduling for file placement and delivery in cache-assisted wireless networks with finite file lifetime. IEEE Transactions on Communications 67(6), 4177-4192. https://doi.org/10.1109/TCOMM.2019.2902150

Martinez-Sanchez D.A. and Jimenez G. (2019). Hydraulic fracturing considerations: Insights from analogue models, and its viability in Colombia. Earth Sciences Research Journal 23(1), 5-15. https://doi.org/10.15446/esrj.v23n1.69760

Matsuda Y., Xie M. and Fujii A. (2018). An integrated experimental and theoretical reaction path search: analyses of the multistage reaction of an ionized diethylether dimer involving isomerization, proton transfer, and dissociation. Physical Chemistry Chemical Physics 20(21), 14331-14338. https://doi.org/10.1039/C7CP08566D

Perazzo P., Sorbelli F.B., Conti M., Dini G. and Pinotti C.M. (2017). Drone path planning for secure positioning and secure position verification. IEEE Transactions on Mobile Computing 16(9), 2478-2493. https://doi.org/10.1109/tmc.2016.2627552

Sundar K., Rathinam S. and Sharma R. (2019). Path planning for unmanned vehicles with localization constraints. Optimization Letters 13(2), 993-1009. https://doi.org/10.1007/s11590-019-01435-8

Takayanagi T., Nakatomi T. and Yonetani Y. (2018). On the ion-pair dissociation mechanisms in the small NaCl•(H2O) 6 cluster: A perspective from reaction path search calculations. Journal of Computational Chemistry 39(23), 1835-1842. https://doi.org/10.1002/jcc.25227

Tan Y.Q., Lu L., Bonde A, Wang D. and Qi J. (2018). Lymph node segmentation by dynamic programming and active contours. Medical Physics 45(5), 2054-2062.https://doi.org/10.1002/mp.12844

Wang S., Zhang K., Beek L.P.H., Tian X. and Bogaard T.A. (2020). Physically-based landslide prediction over a large region: Scaling low-resolution hydrological model results for high-resolution slope stability assessment. Environmental Modelling & Software 124, 104607. https://doi.org/10.1016/j.envsoft.2019.104607

Wang W.K., Wu X.B., Chen and W.B. (2018). Research on path planning of intelligent plant inspection robot. Journal of Computers (Taiwan) 29(2), 174-185. https://doi.org/10.3966/199115992018042902017

Wen F., Zhao Y., Zhang M. and Hu C. (2019). Forecasting realized volatility of crude oil futures with equity market uncertainty. Applied Economics 51(59), 6411-6427. https://doi.org/10.1080/00036846.2019.1619023

Yu D., Mao Y., Gu B., Nojavan S. and Nasseri M. (2020). A new LQG optimal control strategy applied on a hybrid wind turbine/solid oxide fuel cell/ in the presence of the interval uncertainties. Sustainable Energy, Grids and Networks 21, 100296. https://doi.org/10.1016/j.segan.2019.100296

Zhao B., Jia L.H., Xia H.B. and Li Y.C. (2018). Adaptive dynamic programming-based stabilization of nonlinear systems with unknown actuator saturation. Nonlinear Dynamics 93(4), 2089-2103. https://doi.org/10.1007/s11071-018-4309-8

Zuo X., Dong M. and Gao F. (2020). The modeling of the electric heating and cooling system of the integrated energy system in the coastal area. Journal of Coastal Research 103(sp1), 1022. https://doi.org/10.2112/SI103-213.1